Asymptotic Theory of Diffraction by Elongated Bodies — from V. A. Fock to Present

I. V. Andronov[(1)] and R. Mittra[(2)]
[(1)] Dept. of Compuuttional Physics, St.Petersburg State University,
Ulianovskaya 1-1, Petrodvoters, 198504, Russia
(e-mail: iva---@list.ru)
[(2)] Electromagnetic Communication Lab, EE Department, Pennsylvania State University,
319 Electrical Engineering East University Park, PA 16802-2705, USA
(e-mail: rajmittra@ieee.org)

***Abstract*—The problem of high-frequency diffraction by elongated bodies is discussed in this work. The classical approach is shown to require too high frequencies for its applicability. Attempts to improve the approximating properties of the asymptotic methods are discussed, focusing on the case of strongly elongated bodies examined in detail. The asymptotics are governed by the elongation parameter, the ratio of the longitudinal wave dimensions of the body to its cross-section. The cases of axial incidence as that of incidence at a grazing angle to the axis are considered. Both the asymptotics of the induced currents on the surface and of the far field amplitude are developed. Comparison with numerical results for a set of test problems shows that the leading terms of the new asymptotics provide good approximation in a uniform manner with respect to the rate of elongation.**

***Index terms*—High-frequency asymptotics, diffraction, elongated bodies.**

I. Introduction

Methods of high-frequency diffraction remain an important tool for the analysis of wave phenomena in many applications. Classical results of Fock, Keller and others are restricted to geometries in which there is a single large parameter $k\rho$, which measures the characteristic size in wave lengths. The condition of validity of these asymptotic expansions requires that all other quantities describing the problem should not compete with this large parameter. In some cases, this imposes conditions that are too restrictive on the frequency, by requiring it to be very high. One of such cases is the diffraction by elongated bodies.

Interest in high-frequency diffraction developed many years ago to fulfill the needs of numerous applications in radio-engineering. Since computers were not powerful at that time, alternatives to purely numerical analysis were highly appreciated. One of the important advances made on the basis of canonical problems was formulated in terms of the localization principle [1], which made it possible to find solution of diffraction problem for a specific convex body and deduce approximate formulas for the field distribution on its surface. These formulas are also applicable to any other body with the same values of the principal curvatures at a given point. Thus it is possible to decompose the domain occupied by the scatterer into smaller parts and to approximate each part with a canonical problem, whose solution leads to the local asymptotic representations valid in each of the subdomains. The matching of the local expansions is a nontrivial problem, albeit a solvable one as a rule.

Application of the localization principle enabled Fock to find general formulas for the field in the penumbra region by working with the paraboloid of revolution as the particular body [2]. However, the same formulas can be obtained more easily with the help of the parabolic equation method. We will remind the outline of these derivations in the following section, since many of the ideas that form the basis of these derivations remain unchanged in the modern approach to solving the problems of diffraction by elongated bodies.

II. Fock asymptotics

A. The main assumptions

Let us consider the wave field in the near vicinity of the light-shadow boundary on the surface of a convex body. This so-called Fock domain appears to be the cradle of creeping waves that propagate to the shadow region of the boundary, and of the Fresnel transition field in the penumbra region (see Fig. 1).

Our first step is to introduce a coordinate system in which the surface of the body coincides with one of the coordinates surfaces. Usually such a coordinate system is formed by adding the normal to the semi-geodesic coordinates on the surface. That is, we consider a set of geodesics whose directions are defined by the rays of the incident field, and measure the first coordinate s along these geodesics starting from a reference line, which is usually the light-shadow boundary on the surface. The second surface coordinate α just parameterizes the geodesics from this set. In this approach, how the normal coordinate is defined is not important and it can be taken as the geometrical distance to the surface for the case of a general body. However, when dealing with elongated bodies we will return to this question of the choice of the normal coordinate. Once the coordinate system is chosen all the equations and the boundary conditions of the problem should be rewritten in this coordinate system. The

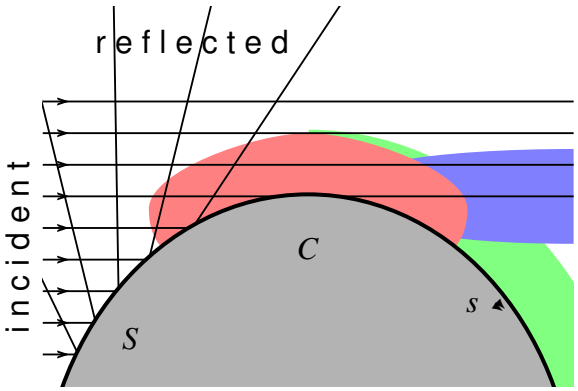

Fig. 1. Diffraction by a convex body. Fock domain – red, Fresnel penumbra – blue, creeping waves – green.

characteristics of the surface and the incident field, such as radius of curvature ρ of the geodesics, their divergence h, radius of transverse curvature ρ_t and the torsion appear in the above equations.

The next step in this procedure is to choose the scales of the coordinates. One should scale the coordinates in a way such that the derivatives of the field by the scaled coordinates can be considered as quantities that are on the order of unity. In our case, the field depends on s in the form of a dominant factor e^{iks}, multiplied by a slower varying function called the attenuation function. To define the scales one can proceed in one of two ways. One possibility is to search for these scales in the solution of a canonical problem, which can be solved exactly. The other possibility is to look at the terms in the equations and to attempt to choose terms that should be considered as the principal ones. We will illustrate this second approach by considering the diffraction by a cylinder as an example. For this 2D problem, Maxwell's equations are reduced to the Helmholtz equation for scalar waves.

Let S be the convex boundary of a body illuminated by a wave field given by its ray expansion. Figure 1 presents the two-dimensional cross-section of the field of rays. On the line C on the surface S (see Fig. 1) the rays of the incident field are tangent to S. Such rays are called limiting rays. The surface is illuminated on one side of C, that is it is reached by incident rays and each incident ray is reflected from S. No geometrical rays reach the surface on the other side.

As mentioned above, our next step is to we introduce the representation

$$U = \exp(iks)u(s,n), \tag{1}$$

and assume that the new unknown function u varies more slowly with the s coordinate than does the exponential multiplier. We substitute the above representation into the equation and rewrite it in terms of the coordinates (s,n) as

$$2ik\frac{\partial u}{\partial s} + \frac{\partial^2 u}{\partial s^2} + \frac{n}{\rho+n}\frac{\rho'}{\rho}\left(iku + \frac{\partial u}{\partial n}\right) + \frac{\partial^2 u}{\partial n^2} + 2\frac{n}{\rho}\frac{\partial^2 u}{\partial n^2} + \frac{n^2}{\rho^2}\frac{\partial^2 u}{\partial n^2} + \frac{1}{\rho}\frac{\partial u}{\partial n} + \frac{n}{\rho^2}\frac{\partial u}{\partial n} + 2k^2\frac{n}{\rho}u + k^2\frac{n^2}{\rho^2}u = 0. \tag{2}$$

Next, we introduce the stretched coordinates

$$k^\alpha s, \qquad k^\beta n$$

where the exponents α and β are unknowns as yet. We assume only that $\alpha < 1$ (otherwise u varies with s faster than the exponential factor in (1)). This assumption enables us to exclude the term $\partial^2 u/\partial s^2$ from principal terms and to consider it as a correction to the term $2ik\partial u/\partial s$. Further, to be able to fix the boundary condition at $n = 0$ and radiation condition at $n = +\infty$ the second-order derivative w.r.t. n should be included in the principal-order terms. This implies that $\beta > 0$ and the terms with $\partial u/\partial n$ are smaller than $\partial^2 u/\partial n^2$. Finally, the n^2 terms are smaller than similar terms with n in the first power. In view of all this the following three terms may be considered to be the principal terms in equation (2) :

$$\frac{\partial^2 u}{\partial n^2}, \qquad 2ik\frac{\partial u}{\partial s}, \quad \text{and} \quad 2k^2\frac{n}{\rho}u. \tag{3}$$

One should verify that all the terms in (3) are principal-order terms, because otherwise the boundary value problems involving n would have no solution. Preserving all three terms yields the well known Leontovich parabolic equation :

$$2ik\frac{\partial u}{\partial s} + \frac{\partial^2 u}{\partial n^2} + 2k^2\frac{n}{\rho}u = 0. \tag{4}$$

Simultaneously, we have determined the size of the Fock domain. Parabolic equation (4) fixes the scales $\alpha = 1/3$ and $\beta = 2/3$. Thus, Fock domain is as small as $k^{-1/3}$ along the surface, and as small as $k^{-2/3}$ in the direction of the normal. For the more complex case of 3D problem, the parabolic equation remains the same, since within such a small domain any general surface is almost cylindrical.

B. Solution of the parabolic equation

In the Fock domain, we can usually replace $\rho(s,\alpha)$ by its value $\rho_0(\alpha)$ on the light-shadow boundary, since the Fock domain is small and $\rho(s,\alpha) \approx \rho_0(\alpha)$. Then the coefficients of the parabolic equation become constant, and it can be solved by means of Fourier transform to get :

$$u = \int_{-\infty}^{+\infty} e^{i\sigma\zeta}\hat{u}(\nu,\zeta)d\zeta, \tag{5}$$

where we have introduced the stretched coordinates

$$\sigma = m\frac{s}{\rho_0}, \qquad \nu = 2m^2\frac{n}{\rho_0}, \qquad m = \left(\frac{k\rho_0}{2}\right)^{1/3}. \tag{6}$$

For $\hat{u}$, we obtain the Airy equation

$$\frac{\partial^2 \hat{u}}{\partial \nu^2} + \Big(\nu - \zeta\Big)\hat{u} = 0. \tag{7}$$

We use the Airy functions v and w_1 in Fock notation. The function w_1 is chosen because it satisfies the radiation condition representing only the waves which propagate away from the surface. The solution can be written as an integral

$$u = \int_{-\infty}^{+\infty} e^{i\sigma\zeta}c(\zeta)\Big(v(\zeta-\nu) + R(\zeta)w_1(\zeta-\nu)\Big)d\zeta. \tag{8}$$

The part of the solution which contains the Airy function $v(\zeta-\nu)$ corresponds to the incident field and the part of the solution which contains the Airy function $w_1(\zeta-\nu)$ represents the secondary field. The coefficient R is determined from the boundary condition. Thus from the Neumann condition, for the TM polarization we find

$$R^{\mathrm{TM}}(\zeta) = -\frac{\dot{v}(\zeta)}{\dot{w}_1(\zeta)}, \tag{9}$$

where dot denotes the derivative. For the TE polarization, by imposing the Dirichlet condition we find that

$$R^{\mathrm{TE}}(\zeta) = -\frac{v(\zeta)}{w_1(\zeta)}. \tag{10}$$

The amplitude $c(\zeta)$ remians undetermined as yet, and it enables us to match the local asymptotics in the Fock domain to the incident field. For that we consider the incident wave and represent it in the stretched coordinates (σ,ν) of the boundary layer. For example, for the case of an incident plane wave we have

$$u^i = u^i(C)\exp\left\{i\left(\sigma\nu - \frac{1}{3}\sigma^3\right)\right\}.$$

By inserting this expression in (8), we obtain the integral equation for the amplitude $c(\zeta)$, which reads

$$\int_{-\infty}^{+\infty} e^{i\sigma\zeta}c(\zeta)v(\zeta-\nu)d\zeta = u^i(C)\exp\left\{i\left(\sigma\nu - \frac{1}{3}\sigma^3\right)\right\}. \tag{11}$$

Applying the Fourier transform we find

$$c(\zeta) = u^i(C)\frac{1}{\sqrt{\pi}}.$$

If σ is large, one can compute the integrals by using the residue theorem. Then, the contribution of every residue matches to the creeping waves which propagate along the surface of the body.

C. Induced currents: leading- and higher-order terms

If we take the observation point in formula (8) on the surface, i.e., if we let $\nu = 0$, we obtain the well known expression for the field associated with the TE-polarized wave

$$E = U^i(C)\frac{e^{iks}}{\sqrt{\pi}}\int_{-\infty}^{+\infty} e^{i\sigma\zeta}\frac{d\zeta}{w_1(\zeta)}. \tag{12}$$

Similarly, for the induced current of the TM wave, we get

$$J = U^i(C)\frac{e^{iks}}{\sqrt{\pi}}\int_{-\infty}^{+\infty} e^{i\sigma\zeta}\frac{d\zeta}{\dot{w}_1(\zeta)}. \tag{13}$$

Although (12) and (13) only contain the leading order terms of the asymptotics, and the asymptotic decomposition is carried out by using the inverse powers of m, i.e., fractional powers of $k\rho$, they yield a rather accurate approximation for the field even when the frequency is not too high. We can verify this from Fig. 2 of [3] (the original is in [4]), where the currents induced on a circular cylinder, whose diameter is equal to the wavelength, have been presented. It is worthwhile to point out that in the diffraction problem the current is formed by the interference of two waves. One travels in the clockwise direction from the light-shadow boundary, while the other originates from the light-shadow boundary on the opposite side of the cylinder and travels in the counter-clockwise direction. Both of these waves are attenuated, but as the diameter of the cylinder is not large, the wave which encircles the shadowed side, does not travel a large distance, and its contribution remains noticeable in the form of the oscillations of the field amplitude.

For an arbitrary (non-cylindrical) 3D surface, the derivations of the principal-order term are exactly as presented above. The second surface coordinate α is not stretched in the Fock domain and derivatives with respect to this coordinate are not involved in the higher-order operator. Because of this, the leading-order term of the asymptotics is not affected by the transverse curvature of the body. However the induced currents are different if the body is a sphere, and the agreement between the real currents and the asymptotics is not so good as it is for the case of the cylinder. A comparison with the numerical results presented in [5] defines the domain of applicability where the results from the Fock formulas suffer from less than 5% error, provided $k\rho > 20$. Attempts to improve the situation entail the computation of the next-order terms of the asymptotics, and we mention here only three papers that have attempted to do this. The first one is by Hong [6], who has derived the second-order term of the asymptotics, both for the fields in the Fock domain and for creeping waves in the deep shadow. He has considered an arbitrary (with some restrictions) smooth convex surface with ideal boundary conditions. For the impedance boundary conditions, the second-order term in the asymptotics of creeping waves was found in [7]. It was possible to find not only the second-order term for the case of a sphere, but the entire series representation [8]. However, the latter result differs by a factor of 2 from the one by Hong. Inspite of the possibility

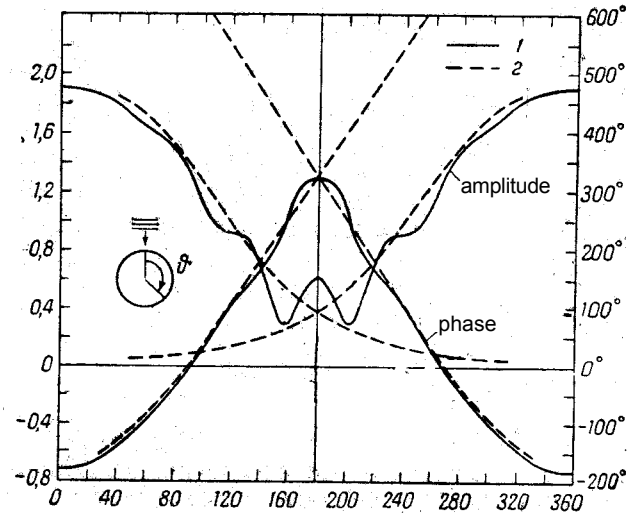

Fig. 2. Currents on a perfectly conducting circular cylinder with the diameter equal to the wavelength. Solid line – exact, dashed – Fock asymptotics (13).

to use the second- and higher-order terms, the lower bound of frequency domain where the asymptotic formulas yield sufficiently accurate representations for the currents on the sphere, have remained almost unchanged. This leads us to conclude that the higher-order terms do not enlarge the domain of applicability of the first-order representation.

III. Moderately and Strongly elongated bodies

For elongated objects, such as spheroids, the lower frequency bound of the domain where Fock formulas can be used shifts to $kb > 100$ and larger. We can deduce this by comparing the principal-order term of the asymptotics with numerical results given in [9]. Figure 3 presents the induced currents on the spheroid with semiaxes $a = 0.5$m and $b = 1.25$m, at frequencies 1, 2 and 4 GHz and the asymptotics. We use the stretched coordinate σ in which the "size" of the spheroid changes with frequency, but the asymptotics remain unchanged. Figure 3 shows that the Fock formula underestimates the values for the currents. This is consistent with the observation that the edges or surfaces with high transverse curvature decrease the attenuation of the creeping waves. That is, large transverse curvature or sharp edges promote the propagation of waves, as exemplified by the following cases. While studying diffraction by disks Senior [10] observed, in 1969, that a wave propagates with low attenuation along the rim of the disk. The Sommerfeld wave [11] propagates with only logarithmic attenuation along conducting wires. Finally, a source on a cylinder excites a wave that propagates along the generatrix of the cylinder, and only decreases as the inverse of the square root of the distance [12].

The impact of transverse curvature on the propagation constant of creeping waves, and more specifically, the case of creeping wave on elongated bodies, has been analyzed in [13] (see also [14]). In the spirit of the work of Engineer *et al.* [15], who have studied the problem of diffraction by 2D slender bodies, it was assumed that besides the usual asymptotic parameter $k\rho$, the geometrical characteristics of the body form another large parameter $\Lambda = \rho/\rho_t$, with which the asymptotic parameter may compete. Analysis of the scales shows that reorganization of the usual creeping waves asymptotics as well as the asymptotics in Fock domain takes place when Λ reaches the order of m, i.e., becomes as large as $(k\rho)^{1/3}$. This case was referred to in [13] as the case of *moderately elongated body*. For this case, the leading term of the asymptotics of creeping waves starts to depend on the transverse curvature, and transverse curvature on the order of $(k\rho)^{1/3}/\rho$ changes the creeping waves asymptotics, although these changes are not too significant. The structure of the asymptotic expansion remains relatively unchanged, though some terms in the recurrent system of the boundary-value problems move from the second-order corrections to the first-order. This results in an aditional multiplier defining the amplitude of creeping waves. This result can be simulated by introducing an effective impedance :

$$Z = \frac{i}{2k\rho_t} \tag{14}$$

which can evidently be used in the Fock domain. The asymptotics of induced currents on a moderately elongated body improves the approximation, as may be seen from Fig. 4. However, the currents still remain underestimated.

The *strongly elongated body* was defined in [13] as the body in which the transverse curvature is on the order of $k^{2/3}\rho^{-1/3}$, implying that $\Lambda \sim m^2$. The asymptotics of creeping waves on such a body changes significantly and leads to the equation below, which is more complex (see [13]) than the Airy equation (7)

$$\frac{\partial^2 \hat{u}}{\partial \nu^2} + \frac{3}{\nu+\kappa}\frac{\partial \hat{u}}{\partial \nu} + \Big(\nu + \kappa - \zeta\Big)\hat{u} = 02, \tag{15}$$

where

$$\kappa = 2m^2\frac{\rho_t}{\rho}. \tag{16}$$

For the case of a strongly elongated body, the parameter κ is on the order of unity and is the main parameter which describes the effect of the transverse curvature. The formulas reduce to the effective impedance approach of moderately elongated case, if we let the parameter κ to be small. Equation (15) is a biconfluent Heun equation [16] which has 4 singular points, three of which coalesce at infinity, while the last one goes to zero. The singularity of $\nu = -\kappa$ in (15) corresponds to the points on the axis of transverse curvature and it is convenient to introduce a "shifted" normal $\nu' = \nu + \kappa$, especially for the case of a body of revolution. Then the surface equation becomes $\nu' = \kappa$. In order to be able to write the asymptotics of creeping waves on a strongly elongated body, it is necessary to impose some restrictions on the variation of both the curvature and the transverse curvature; specifically it is necessary to assume that both ρ and ρ_t vary very slowly.

Attempts to generalize the approach to Fock domain (almost the only published result we can locate is [17]) were neither mathematically rigorous nor satisfactory from the point of view of providing a good approximation for the currents. Although the effect was apparently described correctly at the qualitative level, agreement with the results of numerical computation was less than satisfactory.

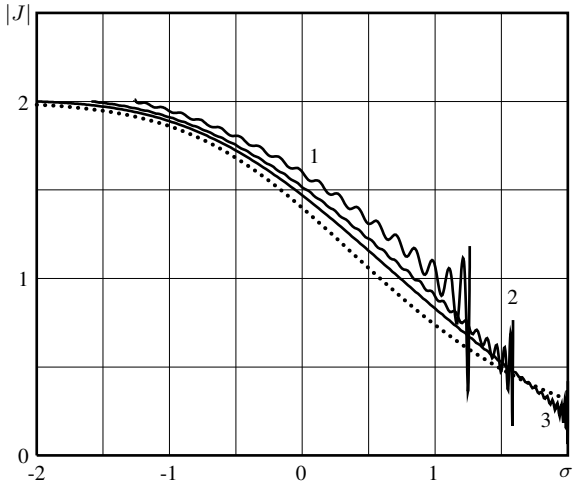

Fig. 3. Induced current amplitude on the spheroid with semiaxes $b = 1.25$ m, $a = 0.5$ m at frequencies 1, 2 and 4 GHz (curves 1,2,3) and the asymptotic approximation by Fock (dotted curve).

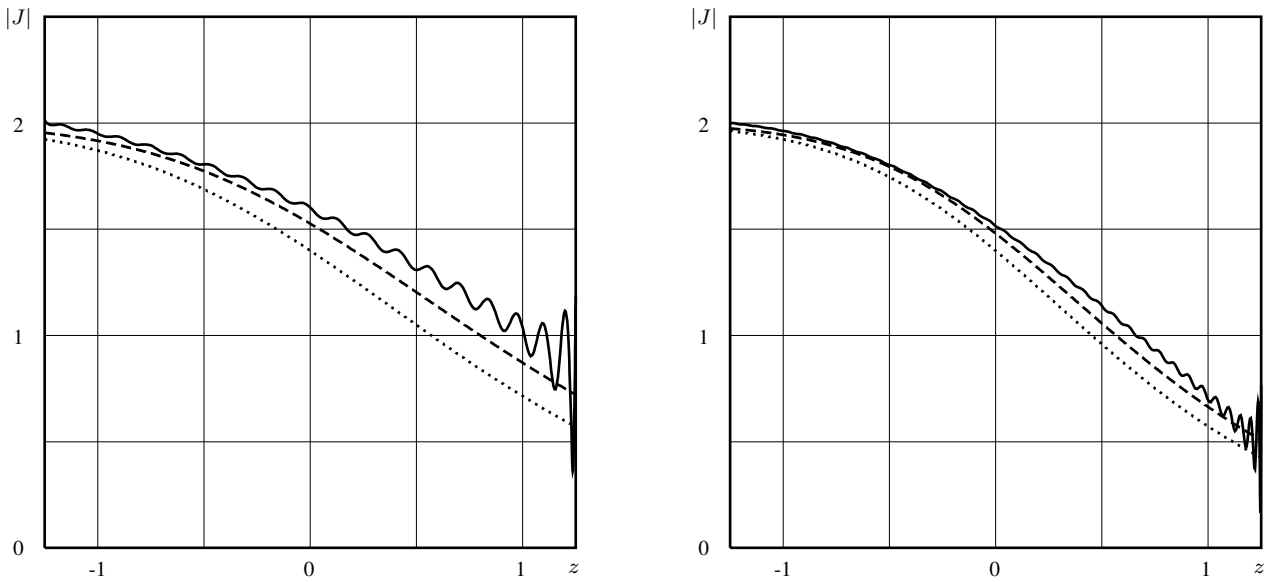

Fig. 4. Moderately elongated body approximation for diffraction by the spheroid with $a = 0.5$m, $b = 1.25$m at 1 GHz (left) and 2 GHz (right). Numerical results – solid, moderately elongated approximation – dashed, Fock approximation – dotted.

It was understood later that the restrictions imposed on the curvature variation were inconsistent with the geometry. Indeed for a very elongated body, such as a prolate spheroid with $\Lambda = O(m^2)$, which is illuminated along its axis by an incident wave, the entire object is not located in the deep shadow region, but in the light-shadow transition zone. Therefore it is not correct to replace it with an object with constant ρ and ρ_t.

All the above-mentioned facts led to the conclusion, which was recently rediscovered in [18], that a different technique is neded to handle the case of strongly elongated body. To address this problem, a new technique was introduced in 2009 [19], [20] which is currently being developed. The rest of the paper describes this new approach.

IV. Diffraction by a strongly elongated body

A. Boundary layer, scales and coordinates

Let the elongated body have the symmetry of revolution and let its main radii of curvature at the widest cross-section be ρ and ρ_t. We assume that the body is spheroid-like, i.e., its surface deviates from the surface of the spheroid by an asymptotically small distance. The radii of curvature define the semiaxes of this spheroid as

$$a = \rho_t, \qquad b = \sqrt{\rho\rho_t}. \tag{17}$$

The assumption that the body be strongly elongated in terms of the semiaxes can be expressed as

$$\chi \equiv \frac{ka^2}{b} = O(1). \tag{18}$$

We refer to the parameter χ as the elongation parameter. It is related to the parameter κ, introduced earlier, via the formula

$$\chi = 2^{-1/2}\kappa^{3/2}.$$

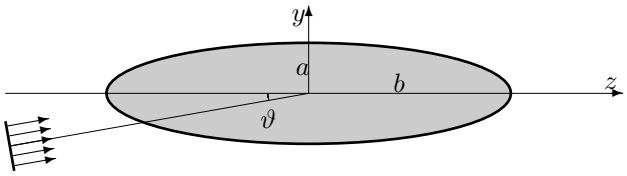

Fig. 5. Geometry of the problem.

We use the spheroidal coordinates (ξ, η, φ) related to the cylindrical (r, z, φ) ones, where the z axis is the axis of the body (see Fig. 5), via the formulas

$$z = p\xi\eta, \qquad r = p\sqrt{\xi^2 - 1}\sqrt{1 - \eta^2}, \tag{19}$$

where $p = \sqrt{b^2 - a^2}$ is the semi-focal distance.

In order to choose the scales, we initially consider the case of a plane wave incident along the axis of the body, and make some generalizations later. If the body were not elongated, we would use Fock asymptotics described in Section II. The size of Fock domain is on the order $(k\rho)^{-1/3}$ in the direction of the wave incidence, while it is on the order $(k\rho)^{-2/3}$ along the normal direction. We see that if we maintin these orders, then the entire strongly-elongated body would be inside the Fock domain, implying that we should not stretch the angular spheroidal coordinate η, but should do so with the radial coordinate ξ. It is convenient to replace ξ with another coordinate, which we denote by τ, such that its value measured from the axis would be on the order of unity on the surface. We introduce such a coordinate by using the formula

$$\tau = 2\chi^{-1}kb(\xi - 1). \tag{20}$$

So that $\tau = 0$ on the axis while it equals 1 on the surface. The coordinates (η, τ) serve as the coordinates of the boundary layer, and they replace the usual σ and ν coordinates of the asymptotics of Fock.

Keeping in mind that $a \ll b$, we can simplify the formulas for the boundary-layer coordinates to

$$\begin{cases} r = a\sqrt{1-\eta^2}\sqrt{\tau}, \\ z = b\eta + \dfrac{a^2}{2b}(\tau - 1)\eta. \end{cases} \tag{21}$$

This change does not influence the asymptotic procedure which pertains to the leading order, although may affect the higher-order corrections, which we ignore however.

For an ordinary (not elongated) body, the use of the parabolic equation method suggests that the factor e^{iks} be separated. Computing the arc-length s on the spheroid is not so easy; however, we can use a simpler factor $e^{ikp\eta}$ or $e^{ikb\eta}$ if we again exploit the fact that $a \ll b$. These factors agree with e^{iks} up to the terms on the order of unity, and we can choose any of them. The formulas become a little more compact if we choose $e^{ikp\eta}$, which we simplify to

$$\exp\left(ikb\eta - \frac{i}{2}\chi\eta\right). \tag{22}$$

Once we have chosen the coordinates and the factor mentioned above, we can go ahead and generalize the problem, by allowing the wave to be incident at an arbitrary angle with respect to the axis. However, the angle should be small, such that the phase shift corresponding to the trajectory of the wave along the geodesics on the surface differ from the phase shift of the multiplier (22) by no more than a quantity on the order of unity, implying that the angle of incidence ϑ should be such that

$$\beta \equiv \sqrt{kb}\vartheta = O(1). \tag{23}$$

Dimensionless quantities χ and β, that are on the order of unity, are the parameters of the asymptotic formulas, which we will derive below.

B. Integral representation of the field

We search for the solution of Maxwell's equations in the form of a Fourier series in terms of the angle φ. For the part of the electromagnetic field which depends on the angle in the form $e^{i\ell\varphi}$, we express all the components of electric and magnetic vectors via the E_φ and H_φ components. Below we denote the Fourier harmonics of these components as E_ℓ and H_ℓ. The functions E_ℓ and H_ℓ are solutions of the system of differential equations, which is cumbersome to handle, although it is standard in spheroidal coordinates. Separation of variables is possible only if $\ell = 0$ [21], and it leads to a representation of the field that utilizes spheroidal functions.

We now extract the dominant factor in (22), and neglect the lower-order terms. For the leading order in terms of the asymptotic parameter kb, we obtain the system of parabolic equations. It can be easily split into two independent equations for the new unknowns as follows :

$$P_\ell(\tau,\eta) = \frac{E_\ell + iH_\ell}{2}, \qquad Q_\ell(\tau,\eta) = \frac{E_\ell - iH_\ell}{2}. \tag{24}$$

These unknowns satisfy the equations

$$L_{\ell-1}P_\ell = 0, \qquad L_{\ell+1}Q_\ell = 0, \tag{25}$$

$$L_n = \tau\frac{\partial^2}{\partial\tau^2} + \frac{\partial}{\partial\tau} + \frac{i\chi}{2}\left(1-\eta^2\right)\frac{\partial}{\partial\eta} + \frac{1}{4}\left(\chi^2\tau - \frac{n^2}{\tau} - \chi^2\left(1-\eta^2\right)\right). \tag{26}$$

The differential equations in (25) are considered together with the boundary conditions. For the case of a perfectly conducting surface, the boundary conditions require that the tangential components of the electric vector be zero on the surface, which leads to the conditions

$$P_\ell(1,\eta) + Q_\ell(1,\eta) = 0, \tag{27}$$

$$\frac{\partial P_\ell(1,\eta)}{\partial\tau} + \frac{1}{2}P_\ell(1,\eta) - \frac{\partial Q_\ell(1,\eta)}{\partial\tau} - \frac{1}{2}Q_\ell(1,\eta) = 0. \tag{28}$$

We also set the radiation conditions at infinity for the secondary field.

Parabolic operator (26) is amenable to a separation of variables. Elementary solution of the equation $L_nU = 0$ can be written in the form

$$U_n = \frac{1}{\sqrt{\tau}\sqrt{1-\eta^2}}\left(\frac{1-\eta}{1+\eta}\right)^{\mu} F_{\mu,n/2}\left(-i\chi\tau\right), \tag{29}$$

where $F_{\mu,n/2}(g)$ is a solution of the Whittaker equation [22]

$$F'' + \left(-\frac{1}{4} + \frac{\mu}{g} + \frac{1-n^2}{4g^2}\right)F = 0.$$

We choose the Whittaker functions $M_{\mu,n/2}(-i\chi\tau)$ for the incident field in (29). These functions are regular at $\tau = 0$, which results in solutions that are regular in the entire space. For the secondary field, we choose Whittaker functions $W_{\mu,n/2}(-i\chi\tau)$ which correspond to solutions satisfying the radiation condition in terms of τ.

We combine P_ℓ and Q_ℓ of the elementary solutions (29) in the form of integrals over the separation parameter μ. In these representations we include amplitude factors that are dependent on μ. To define the path of integration, and the amplitude factors, we consider below the incident field first.

C. Representation of the incident field

An arbitrarily polarized plane electromagnetic wave can be represented as a sum of transverse electric (TE) and transverse magnetic (TM) waves. We define the transverse direction with respect to the plane of incidence and assume that it coincides with the XOZ plane in Cartesian coordinates (see Fig. 5). The plane of incidence is not defined for the axial case, but TE and TM waves can still be defined with respect to the plane XOZ.

Let us consider the TE case first. We set a unit amplitude for the incident TE wave and express its $\mathbf{E}$ and $\mathbf{H}$ fields as

$$\mathbf{E}^i = \exp\left(ikz\cos\vartheta + ikx\sin\vartheta\right)\mathbf{e}_y, \tag{30}$$

$$\mathbf{H}^i = \exp\left(ikz\cos\vartheta + ikx\sin\vartheta\right)\left\{-\cos\vartheta\mathbf{e}_x + \sin\vartheta\mathbf{e}_z\right\}, \tag{31}$$

where $\mathbf{e}_x$, $\mathbf{e}_y$ and $\mathbf{e}_z$ are the unit vectors of Cartesian coordinates. Next, we represent the incident wave in the form of a

Fourier series as follows :

$$E^i_\varphi = \exp(ikz\cos\vartheta)\left\{ iJ_1(kr\sin\vartheta) + 2\sum_{n=1}^{\infty} i^{n-1}\dot{J}_n(kr\sin\vartheta)\cos(n\varphi)\right\}, \quad (32)$$

$$H^i_\varphi = 2\exp(ikz\cos\vartheta)\cos\vartheta\sum_{n=1}^{\infty} i^{n-1}n\frac{J_n(kr\sin\vartheta)}{kr\sin\vartheta}\sin(n\varphi). \quad (33)$$

Each of the harmonics of (32), (33) can be expanded in an asymptotic series in terms of inverse powers of kb. The leading order terms satisfy the parabolic equations (25). Therefore the leading order terms in the asymptotic representation of (32), (33) can be represented as a combination of elementary solutions (29) in which, as explained above, we should include the Whittaker function $M_{\mu,n/2}(-i\chi\tau)$. Expressions for the harmonics in (32) and (33) contain the derivatives of Bessel functions and the ratios of Besel functions to their agument. However both these expressions can be reduced to just the Bessel functions with the help of the formulas :

$$2\dot{J}_n(g) = J_{n-1}(g) - J_{n+1}(g),$$
$$2n\frac{J_n(g)}{g} = J_{n-1}(g) + J_{n+1}(g)$$

from [22]. Therefore the problem of finding the leading-order representation of the incident wave as a combination of the elementary solutions (29) reduces to that of finding such a representation for the functions

$$\exp(ikz\cos\vartheta)\,J_n(kr\sin\vartheta).$$

When substituting here the expressions for the coordinates r and z we replace the trigonometric functions of small ϑ by their approximations : $\sin\vartheta \approx \vartheta$ and $\cos\vartheta \approx 1 - \frac{1}{2}\vartheta^2$. By doing this, we obtain the equation

$$\frac{1}{\sqrt{\tau}\sqrt{1-\eta^2}}\int\left(\frac{1-\eta}{1+\eta}\right)^{\mu} A_n(\mu)M_{\mu,n/2}(-i\chi\tau)d\mu = = V(\eta,\tau). \quad (34)$$

Both the left-hand as well as the right-hand side of this equation satisfy the parabolic equation with operator L_n. Therefore, if we find the amplitude $A_n(\mu)$ for any fixed τ, it will satisfy (34) for all other values of τ. This important property simplifies the problem of finding the solution. First, we rewrite (34) in the form

$$\frac{1}{\sqrt{\chi\tau}\beta\sqrt{1-\eta^2}}\int\left(\frac{1-\eta}{1+\eta}\right)^{\mu}\Omega_n(\mu)M_{\mu,n/2}(i\beta^2)\times \times M_{\mu,n/2}(-i\chi\tau)d\mu = V(\eta,\tau), \quad (35)$$

where

$$A_n(\mu) = \frac{M_{\mu,n/2}(-i\beta^2)}{\sqrt{\chi}\,\beta}\Omega_n(\mu). \quad (36)$$

We note that τ is presented in (35) only as the product $\chi\tau$. Thus, since Ω_n does not depend on τ, it does not depend on χ either. Further, since $\chi\tau$ and $-\beta^2$, presented in (35), are symmetric, Ω_n does not depend on β either. This enables us to find Ω_n for any chosen $\chi\tau$ and β. Equation (35) takes the simplest form if β and $\chi\tau$ both $\to 0$. Computing this limit and using the asymptotics

$$M_{\mu,n/2}(g) \sim g^{(1+n)/2}, \qquad g\to 0, \quad (37)$$
$$J_n(g) \sim \frac{1}{n!}\left(\frac{g}{2}\right)^n, \qquad g\to 0$$

we reduce equation (35) to

$$\int\left(\frac{1-\eta}{1+\eta}\right)^{\mu}\Omega_n(\mu)d\mu = \frac{1}{2^n n!}\left(1-\eta^2\right)^{(n+1)/2}. \quad (38)$$

We remind that we have not yet chosen the path of integration. So if we choose it now as the imaginary axis and set

$$\eta = \frac{s-1}{s+1},$$

equation (38) reduces to

$$\int_{-i\infty}^{+i\infty} s^{-\mu}\Omega_n(\mu)d\mu = \frac{2}{n!}\left(\frac{\sqrt{s}}{s+1}\right)^{n+1}.$$

We identify the left-hand side of this equation with inverse Mellin transform and find

$$\Omega_n(\mu) = \frac{1}{\pi(n!)^2}\Gamma\left(\frac{n+1}{2}+\mu\right)\Gamma\left(\frac{n+1}{2}-\mu\right). \quad (39)$$

Using (39) we can write the incident plane TE wave in the form :

$$E^i_\varphi = -i\frac{\exp(ikb\eta - i\chi\eta/2)}{\sqrt{1-\eta^2}\beta\sqrt{\chi\tau}}\int_{-\infty}^{+\infty}\left(\frac{1-\eta}{1+\eta}\right)^{it}\times \times\left\{-\Omega_1(it)M_{it,\frac{1}{2}}(-i\chi\tau)M_{it,1/2}(i\beta^2) + \sum_{\ell=1}^{+\infty} i^\ell\cos(\ell\varphi)\left[\Omega_{\ell-1}(it)M_{it,\frac{\ell-1}{2}}(-i\chi\tau)M_{it,\frac{\ell-1}{2}}(i\beta^2) - \Omega_{\ell+1}(it)M_{it,\frac{\ell+1}{2}}(-i\chi\tau)M_{it,\frac{\ell+1}{2}}(i\beta^2)\right]\right\}dt, \quad (40)$$

$$H^i_\varphi = -i\frac{\exp(ikb\eta - i\chi\eta/2)}{\sqrt{1-\eta^2}\beta\sqrt{\chi\tau}}\int_{-\infty}^{+\infty}\left(\frac{1-\eta}{1+\eta}\right)^{it}\times \times\sum_{\ell=1}^{+\infty} i^\ell\sin(\ell\varphi)\left[\Omega_{\ell-1}(it)M_{it,\frac{\ell-1}{2}}(-i\chi\tau)M_{it,\frac{\ell-1}{2}}(i\beta^2) + \Omega_{\ell+1}(it)M_{it,\frac{\ell+1}{2}}(-i\chi\tau)M_{it,\frac{\ell+1}{2}}(i\beta^2)\right]dt. \quad (41)$$

The representations for the TM plane wave

$$\mathbf{E}^i = \exp(ikz\cos\vartheta + ikx\sin\vartheta)\left\{\cos\vartheta\mathbf{e}_x - \sin\vartheta\mathbf{e}_z\right\},$$
$$\mathbf{H}^i = \exp(ikz\cos\vartheta + ikx\sin\vartheta)\,\mathbf{e}_y$$

can be derived analogously. The electric field is given by the expression (41) and the magnetic field can be expressed as in (40) with the opposite sign.

D. Boundary conditions and the induced currents

The representations for the secondary fields are similar to (40) and (41), the only change being the replacement of Whittaker functions $M_{it,n}(-i\chi\tau)$ with the functions $W_{it,n}(-i\chi\tau)$, multiplied by a function of the integration variable t. Note that the Whittaker functions $W_{it,n}(-i\chi\tau)$ are chosen because they satisfy the radiation condition. For the TE case we have, in accordance with (24) and (25),

$$E_\varphi^s = -i\frac{\exp(ikb\eta - i\chi\eta/2)}{\sqrt{1-\eta^2}\beta\sqrt{\chi\tau}}\int\limits_{-\infty}^{+\infty}\left(\frac{1-\eta}{1+\eta}\right)^{it}\times$$
$$\times\left\{-\Omega_1(it)T_0(t)W_{it,\frac{1}{2}}(-i\chi\tau)M_{it,\frac{1}{2}}(i\beta^2)\right.$$
$$+\sum_{\ell=1}^{+\infty} i^\ell\cos(\ell\varphi)\left[\Omega_{\ell-1}(it)R_\ell(t)W_{it,\frac{\ell-1}{2}}(-i\chi\tau)M_{it,\frac{\ell-1}{2}}(i\beta^2)\right.$$
$$\left.\left.-\Omega_{\ell+1}(it)T_\ell(t)W_{it,\frac{\ell+1}{2}}(-i\chi\tau)M_{it,\frac{\ell+1}{2}}(i\beta^2)\right]\right\}dt, \tag{42}$$

$$H_\varphi^s = -i\frac{\exp(ikb\eta - i\chi\eta/2)}{\sqrt{1-\eta^2}\beta\sqrt{\chi\tau}}\int\limits_{-\infty}^{+\infty}\left(\frac{1-\eta}{1+\eta}\right)^{it}\times$$
$$\times\sum_{\ell=1}^{+\infty} i^\ell\sin(\ell\varphi)\left[\Omega_{\ell-1}(it)R_\ell(t)W_{it,\frac{\ell-1}{2}}(-i\chi\tau)M_{it,\frac{\ell-1}{2}}(i\beta^2)\right.$$
$$\left.+\Omega_{\ell+1}(it)T_\ell(t)W_{it,\frac{\ell+1}{2}}(-i\chi\tau)M_{it,\frac{\ell+1}{2}}(i\beta^2)\right]dt. \tag{43}$$

The functions $R_\ell(t)$ and $T_\ell(t)$, introduced herein, play the role of the reflection coefficients in some sense, and can be found when the sum of the incident and secondary fields is substituted in the boundary conditions (27), (28). Evidently, each of the harmonics satisfies the boundary conditions separately. For the TE case, we find (for details of the derivations see [23]) :

$$T_0 = -\frac{M_{it,1/2}(-i\chi)}{W_{it,1/2}(-i\chi)}, \tag{44}$$

$$T_\ell = -\frac{Y_{\ell-1,\ell+1}}{Z_\ell} - \frac{1}{Z_\ell}\frac{\mathcal{W}_{(\ell-1)/2}}{C_\ell}, \qquad \ell = 1,2,\dots \tag{45}$$

$$R_\ell = -\frac{Y_{\ell+1,\ell-1}}{Z_\ell} - \frac{1}{Z_\ell}\mathcal{W}_{(\ell+1)/2}C_\ell, \qquad \ell = 1,2,\dots \tag{46}$$

where

$$C_\ell = \frac{\ell^2+4t}{2\ell^2(\ell+1)^2}\frac{M_{it,(\ell+1)/2}(i\beta^2)}{M_{it,(\ell-1)/2}(i\beta^2)},$$

$$Y_{n,m} = W_{it,\frac{n}{2}}(-i\chi)\dot{M}_{it,\frac{m}{2}}(-i\chi) + \dot{W}_{it,\frac{n}{2}}(-i\chi)M_{it,\frac{m}{2}}(-i\chi).$$

$$Z_n = W_{i\lambda,\frac{n-1}{2}}(-i\chi)\dot{W}_{i\lambda,\frac{n+1}{2}}(-i\chi) + \dot{W}_{i\lambda,\frac{n-1}{2}}(-i\chi)W_{i\lambda,\frac{n+1}{2}}(-i\chi)$$

and $\mathcal{W}_n$ is the Wronskian of Whittaker functions [22]

$$\mathcal{W}_n = \dot{M}_{it,n}(g)W_{it,n}(g) - M_{it,n}(g)\dot{W}_{it,n}(g) = \frac{\Gamma(1+2n)}{\Gamma(1/2+n-it)}. \tag{47}$$

For the TM case, the formulas are similar. For this case, E_φ is given by the right-hand side of (43) while H_φ is given by the right-hand side of (42), with the common multiplier (-1). The reflection coefficients in these two formulas are as follows:

$$T_0 = -\frac{\dot{M}_{it,1/2}(-i\chi)}{\dot{W}_{it,1/2}(-i\chi)} \tag{48}$$

and the other coefficients T_ℓ, $\ell = 1,2,\dots$ and coefficients R_ℓ are defined by formulas (45) and (46), respectively, but with $C_{\ell\pm1}$ replaced with $-C_{\ell\pm1}$.

The expressions given in (40) through (43) describe the electromagnetic fields in the boundary layer near the surface of the spheroid. In contrast to the classical Fock asymptotics, they do not have locality with respect to the transverse surface coordinate. Indeed, by restricting our analysis to the bodies of revolution we obtained the Fourier series in terms of the transverse angular coordinate φ. In other respects, the structure of these set of formulas has some similarity with the classical asymptotics of the field in the Fock domain. For example, the Fourier integral in ζ in the classical asymptotics is replaced by another integral transform, and the Airy function $v(\zeta-\nu)$ which represents the incident plane wave in (8) is replaced with the Whittaker function $M_{it,n}(-i\chi\tau)$. The Airy function $w_1(\zeta-\nu)$ which represents the secondary wave outgoing from the surface is replaced with the Whittaker function $W_{it,n}(-i\chi\tau)$. The reflection coefficients (9) and (10) became more compex and are given by the expressions in (44) through (46), and (48).

The induced currents $\mathbf{J} = \mathbf{n}\times\mathbf{H}|_{\tau=1}$ can be found by using (40) through (43), with its principal component directed along η. After simple manipulations we can obtain

$$J = e^{ikb\eta}A(\eta,\chi,\beta,\varphi), \tag{49}$$

where

$$A^{\mathrm{TE}}(\eta,\chi,\beta,\varphi) = -\frac{2}{\pi}\frac{e^{-i\chi\eta/2}}{\sqrt{1-\eta^2}\sqrt{\chi}\beta}\times$$
$$\times\int\limits_{-\infty}^{+\infty}\left(\frac{1-\eta}{1+\eta}\right)^{it}\sum_{\ell=1}^{\infty}\frac{i^{\ell-1}\sin(\ell\varphi)}{(\ell+1)!Z_\ell}\times$$
$$\times\left\{\Gamma\left(\frac{\ell}{2}+1+i\lambda\right)M_{it,\frac{\ell+1}{2}}(i\beta^2)W_{it,\frac{\ell-1}{2}}(-i\chi)\right.$$
$$\left.+\ \ell(\ell+1)\Gamma\left(\frac{\ell}{2}+it\right)M_{it,\frac{\ell-1}{2}}(i\beta^2)W_{it,\frac{\ell+1}{2}}(-i\chi)\right\}dt$$

in the TE case.

It is also convenient to represent the special function A^{TE} in terms of the Coulomb wave functions F and H^+ [22], and to use the program developed in [24] for their computation.

Using the formulas

$$M_{it,\frac{\ell+1}{2}}(i\beta^2) = \frac{2ie^{i\pi\ell/4+\pi t/2}\Gamma(\ell+2)}{\sqrt{\Gamma(\ell/2+1+it)\Gamma(\ell/2+1-it)}}F_{\frac{\ell}{2}}\left(t,\frac{\beta^2}{2}\right),$$

$$W_{it,\frac{\ell-1}{2}}(-i\chi) = -ie^{i\pi\ell/4+\pi t/2}\sqrt{\frac{\Gamma(\ell/2+it)}{\Gamma(\ell/2-it)}}H^+_{\frac{\ell}{2}-1}\left(-t,\frac{\chi}{2}\right)$$

we obtain

$$A^{\mathrm{TE}} = \frac{-8e^{-i\chi\eta/2}}{\pi\sqrt{1-\eta^2}\sqrt{\chi}\beta}\int\limits_{-\infty}^{+\infty}\left(\frac{1-\eta}{1+\eta}\right)^{it}\sum_{\ell=1}^{\infty}i^{\ell}\sin(\ell\varphi)\times \times\frac{F_{\frac{\ell}{2}}\left(t,\frac{\beta^2}{2}\right)H^+_{\frac{\ell-2}{2}}\left(-t,\frac{\chi}{2}\right)+F_{\frac{\ell-2}{2}}\left(t,\frac{\beta^2}{2}\right)H^+_{\frac{\ell}{2}}\left(-t,\frac{\chi}{2}\right)}{H^+_{\frac{\ell-2}{2}}\left(-t,\frac{\chi}{2}\right)\dot{H}^+_{\frac{\ell}{2}}\left(-t,\frac{\chi}{2}\right)+\dot{H}^+_{\frac{\ell-2}{2}}\left(-t,\frac{\chi}{2}\right)H^+_{\frac{\ell}{2}}\left(-t,\frac{\chi}{2}\right)}dt. \tag{50}$$

Similarly, for the TM case we can obtain

$$A^{\mathrm{TM}}(\eta,\chi,\beta,\varphi) = \frac{8e^{-i\chi\eta/2}}{\pi\sqrt{1-\eta^2}\sqrt{\chi}\beta}\times \times\int\limits_{-\infty}^{+\infty}\left(\frac{1-\eta}{1+\eta}\right)^{it}\left\{\frac{1}{2}\frac{F_0\left(t,\frac{\beta^2}{2}\right)}{\dot{H}^+_0\left(-t,\frac{\chi}{2}\right)}+\sum_{\ell=1}^{\infty}i^{\ell}\cos(\ell\varphi)\times \times\frac{F_{\frac{\ell}{2}}\left(t,\frac{\beta^2}{2}\right)H^+_{\frac{\ell-2}{2}}\left(-t,\frac{\chi}{2}\right)-F_{\frac{\ell-2}{2}}\left(t,\frac{\beta^2}{2}\right)H^+_{\frac{\ell}{2}}\left(-t,\frac{\chi}{2}\right)}{H^+_{\frac{\ell-2}{2}}\left(-t,\frac{\chi}{2}\right)\dot{H}^+_{\frac{\ell}{2}}\left(-t,\frac{\chi}{2}\right)+\dot{H}^+_{\frac{\ell-2}{2}}\left(-t,\frac{\chi}{2}\right)H^+_{\frac{\ell}{2}}\left(-t,\frac{\chi}{2}\right)}\right\}dt. \tag{51}$$

It is worth noting that one should consider the limit as $\beta\to 0$ for the case of axial incidence. Only the Coulomb wave function $F_{\frac{-1}{2}}$ has a non-zero contribution in this case and the special functions A^{TE} and A^{TM} simplify to

$$A^{\mathrm{TE}}(\eta,\chi,0,\varphi) = A(\eta,\chi)\sin\varphi,$$
$$A^{\mathrm{TM}}(\eta,\chi,0,\varphi) = A(\eta,\chi)\cos\varphi,$$

where

$$A(\eta,\chi) = -\frac{4e^{-i\chi\eta/2}}{\sqrt{\pi\chi}\sqrt{1-\eta^2}}\int\limits_{-i\infty}^{+i\infty}\left(\frac{1-\eta}{1+\eta}\right)^{it}\frac{e^{-\pi t/2}}{\sqrt{\cosh(\pi t)}}\times \times\frac{H^+_{1/2}\left(-t,\frac{\chi}{2}\right)\,dt}{H^+_{-\frac{1}{2}}\left(-t,\frac{\chi}{2}\right)\dot{H}^+_{\frac{1}{2}}\left(-t,\frac{\chi}{2}\right)+\dot{H}^+_{-\frac{1}{2}}\left(-t,\frac{\chi}{2}\right)H^+_{\frac{1}{2}}\left(-t,\frac{\chi}{2}\right)}. \tag{52}$$

The expressions in (50), (51) and (52) are more cumbersome in comparison to the classical Fock functions (13). However, with the help of the program from [24] their computation are relatively straightforward. The integrals converge quite rapidly and only a small interval contributes to the integral. As shown in [9] the function A reduces to the Fock function (13), when $\chi\to+\infty$.

E. Backward wave

The total field in the boundary layer near the surface is the sum of the primary wave running in the positive direction of z together with waves that are formed when the primary wave encircles the ends of the spheroid. The asymptotics in (50) and (51) only describe the primary wave and are valid in the middle part of the spheroid. The reflected backward wave representation in the boundary layer can be written by noting that the backward wave runs in the opposite direction and that there is no incident backward wave. For the case of the axial incidence, considered in [25], the representation of the current corresponding to the backward wave is given by

$$J_b^{\mathrm{TE}} = e^{-ikb\eta}B(\eta,\chi)\sin\varphi,\quad J_b^{\mathrm{TM}} = e^{-ikb\eta}B(\eta,\chi)\cos\varphi,$$

where

$$B(\eta,\chi) = -\frac{4e^{i\chi\eta/2}}{\sqrt{\pi\chi}\sqrt{1-\eta^2}}\int\limits_{-i\infty}^{+i\infty}\left(\frac{1+\eta}{1-\eta}\right)^{it}\frac{e^{-\pi t/2}}{\sqrt{\cosh(\pi t)}}\times \times\frac{H^+_{1/2}\left(-t,\frac{\chi}{2}\right)r(t)\,dt}{H^+_{-\frac{1}{2}}\left(-t,\frac{\chi}{2}\right)\dot{H}^+_{\frac{1}{2}}\left(-t,\frac{\chi}{2}\right)+\dot{H}^+_{-\frac{1}{2}}\left(-t,\frac{\chi}{2}\right)H^+_{\frac{1}{2}}\left(-t,\frac{\chi}{2}\right)}. \tag{53}$$

The special function B is defined by the expression similar to the one given in (52) in which we change the sign of η and introduce an additional multiplier $r(t)$. The latter may be interpreted as the reflection coefficient from the tip of the spheroid. To find this multiplier one needs to construct the field in the vicinity of the spheroid tip, that is for $\eta\approx 1$, and match the sum $J+J_b$ with that field. The difficulty is that there is no asymptotic parameter in the region near the tip of the spheroid. Indeed, the radius of curvature of the surface at the tip is $\rho_e = a^2/b$. Therefore the parameter $k\rho_e$, which is equal to the elongation parameter χ, is on the order of unity. However, there is a way to circumvent this difficulty, as shown in [25], which is based on the observation that a very elongated ellipse, such as a trajectory of a point mass in the central field of the gravity, is well approximated by a parabola. Hence, if we replace the surface of the spheroid by the surface of the paraboloid defined by the equation

$$r^2 = 2\frac{a^2}{b}(b-z),$$

we can use the exact solution of Fock [2] to approximate the field. Matching this Fock solution to the sum of the forward and backward waves allows the reflection coefficient to be found

$$r(t) = ie^{2ikb-i\chi}\frac{\Gamma(1/2+it)}{\Gamma(1/2-it)}\sqrt{\frac{2t-i}{2t+i}}(4kb)^{-2it}. \tag{54}$$

We note that the asymptotic parameter kb is presented in (54) and, rigorously speaking, the formula requires further asymptotic simplifications in the process of computing the integral in (53), as the contribution of the residues in the zeros of the denominator

$$H^+_{-\frac{1}{2}}\left(-t,\frac{\chi}{2}\right)\dot{H}^+_{\frac{1}{2}}\left(-t,\frac{\chi}{2}\right) + \dot{H}^+_{-\frac{1}{2}}\left(-t,\frac{\chi}{2}\right)H^+_{\frac{1}{2}}\left(-t,\frac{\chi}{2}\right) = 0. \tag{55}$$

TABLE I
TEST PROBLEMS PARAMETERS.

no.	f(GHz)	a (m)	b (m)	χ	kb
1	1	0.5	1.25	4.19169	26.19806
1	2	0.5	1.25	8.38338	52.39613
2	1	0.5	1.76776695	2.96397	37.04966
2	2	0.5	1.76776695	5.92795	74.09931
3	1	0.3125	1.39754249	1.46452	29.29032
3	2	0.3125	1.39754249	2.92903	58.58065

Solutions of equation (55) lie in the lower complex half-plane of t (see [20] where solutions of (55) are analyzed) and the main contribution to (53) is due to the residue in the pole with the maximal imaginary part of t. However, finding the solutions of the dispersion equation (55) is not easy, and we compute the integral directly instead. Moreover, we expect that the formulas can also be applied in the case of values of kb, that are not too large, say $kb \approx 3$, when the approximation with one residue fails.

To illustrate the approximating nature of the asymptotic formulas we present the Figs. 6 through 8 taken from the paper in [25]. These figures present the currents induced by the axially incident plane wave on the surface of perfectly conducting spheroids. The trigonometric multiplier of φ is not considered. The parameters of the test examples are presented in Table I. The results computed by the Finite Element Method (FEM) are plotted in red and the asymptotic results are shown in blue. We see that the agreement is quite good and it is better for spheroids with larger elongations. This was expected, because the fact that spheroid is strongly elongated was used, when deriving our asymptotic formulas, in all the derivations and the terms that are small for elongated spheroids were neglected.

For $\vartheta \neq 0$, backward wave asymptotics can be found by using the same approach, but this has not been done, as yet.

F. The far field asymptotics

Since we have been able to obtain a good approximation of the induced currents, the use of the Stratton-Chu formula in [26] enables us to derive the scattered fields. Since the tangential components of the electric vector E are zero on the surface of perfect conductor, this formula reduces to

$$\mathbf{H}^s = -\frac{1}{4\pi}\iint \mathbf{J}\times\nabla G dS, \tag{56}$$

where $\mathbf{J}$ is the total induced current, $\times$ denotes the vector product and G is the scalar Green's function

$$G(\mathbf{r},\mathbf{r}_0) = \frac{e^{ik|\mathbf{r}-\mathbf{r}_0|}}{|\mathbf{r}-\mathbf{r}_0|}.$$

Moving the observation point $\mathbf{r}_0$ in (56) to infinity along the ray defined by the spherical coordinates ϑ_0 and φ_0 we compute the limit under the integration sign to obain the formula for the far field amplitude of the magnetic field, which reads

$$\mathbf{\Psi} = -\frac{1}{4\pi}\iint \mathbf{J}\times\nabla\psi dS. \tag{57}$$

Here ψ is the far field amplitude of G. In view of the reciprocity principle, the formula for ψ in the boundary layer near the surface coincides with the expression for the field of a plane wave incident from the opposite direction. Consequently, we need to replace η by $-\eta$ and φ by $\pi-\varphi$ in (34). This leads to the asymptotic representations

$$\psi = \frac{1}{2}\psi_0 + \sum_{m=1}^{+\infty}\psi_m\cos[m(\varphi-\varphi_0)], \tag{58}$$

$$\psi_m = \frac{2i^{m+1}e^{-ikb\eta+i\chi\eta/2}}{\sqrt{1-\eta^2}\sqrt{\tau}}\times \\ \times\int_{-\infty}^{+\infty}\left(\frac{1+\eta}{1-\eta}\right)^{is}A_m(is,\beta_0)M_{is,\frac{m}{2}}(-i\chi\tau)ds, \tag{59}$$

where $\beta_0 = \sqrt{kb}\vartheta_0$ is the scaled observation angle, and the amplitudes A_m are defined by (36) and (39).

Our goal is to find the leading order asymptotics of $\mathbf{\Psi}$. Towards this end we substitute the asymptotics of the currents in (57) from the previous section.

We use the Cartesian components of the vectors, but perform the integration in the coordinates of the boundary layer, where

$$dS = b\,d\eta\;a\sqrt{1-\eta^2}\,d\varphi.$$

The expression (57) for the x- and y-componets read

$$\Psi_x = -\frac{1}{4\pi}\iint\left(J_y\frac{\partial\psi}{\partial z} - J_z\frac{\partial\psi}{\partial y}\right)dS,$$

$$\Psi_y = -\frac{1}{4\pi}\iint\left(J_z\frac{\partial\psi}{\partial x} - J_x\frac{\partial\psi}{\partial z}\right)dS.$$

The unit vector along the η coordinate almost coincides with the unit vector along z, that is $J_z = J_\eta$ in the leading order, but the correction produces the J_r component

$$J_r = -\frac{a}{b}\frac{\eta}{\sqrt{1-\eta^2}}J_\eta.$$

Using the fact that $J_\eta = H_\varphi$, $J_\varphi = -H_\eta$ and the expression

$$H_\eta = \frac{-i}{\sqrt{kb\chi\tau}\sqrt{1-\eta^2}}\left(2\tau\frac{\partial E_\varphi}{\partial\tau} + E_\varphi + \frac{\partial H_\varphi}{\partial\varphi}\right). \tag{60}$$

it is relatively straightforward to get

$$J_z = H_\varphi, \qquad J_r = -\frac{a}{b}\frac{\eta}{\sqrt{1-\eta^2}}H_\varphi,$$

$$J_\varphi = \frac{i}{ka\sqrt{1-\eta^2}}\left(2\frac{\partial E_\varphi}{\partial\tau} - \frac{\partial H_\varphi}{\partial\varphi}\right)$$

with the Cartesian components defined by

$$J_x = J_r\cos\varphi - J_\varphi\sin\varphi, \qquad J_y = J_r\sin\varphi + J_\varphi\cos\varphi.$$

Let us now consider the gradient of ψ. The differentiation by z in the leading order reduces to the multiplication by $-ik$ and the other derivatives can be expressed by the formulae

$$\frac{\partial\psi}{\partial x} = \frac{1}{a\sqrt{1-\eta^2}}\left(\left(2\frac{\partial\psi}{\partial\tau} - i\chi\eta\psi\right)\cos\varphi - \frac{\partial\psi}{\partial\varphi}\sin\varphi\right),$$

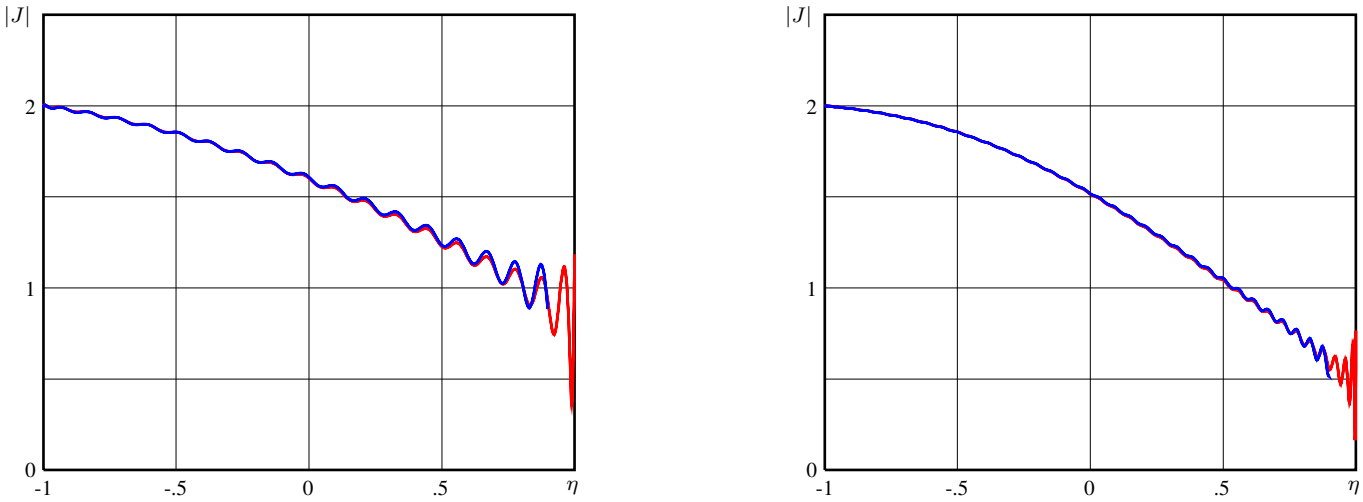

Fig. 6. Amplitudes of the induced current on the spheroid no. 1 (FEM – red, asymptotics – blue).

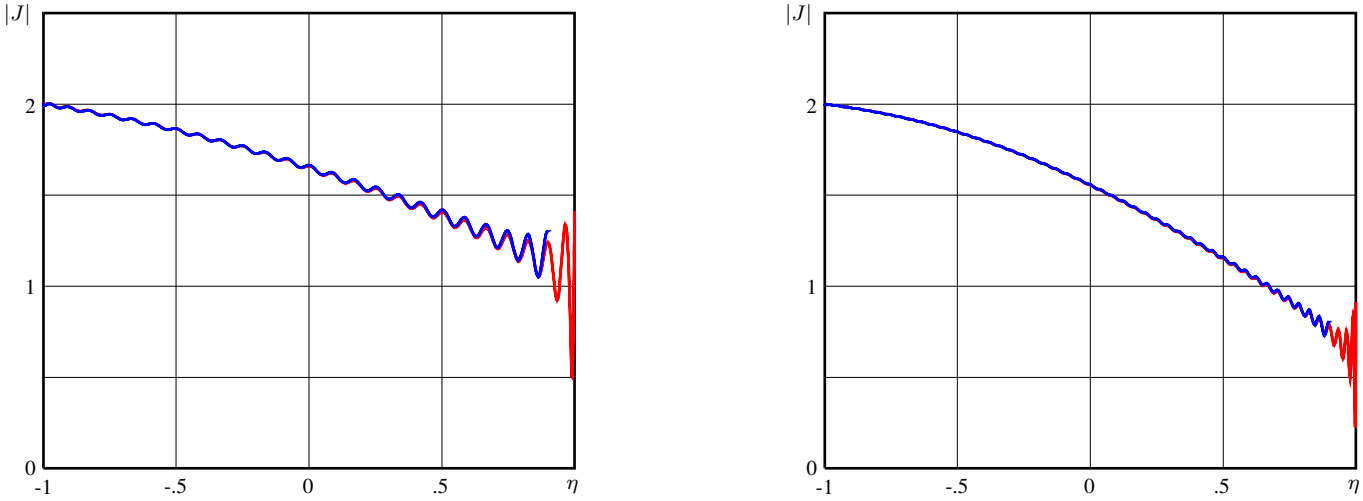

Fig. 7. Amplitudes of the induced current on the spheroid no. 2 (FEM – red, asymptotics – blue).

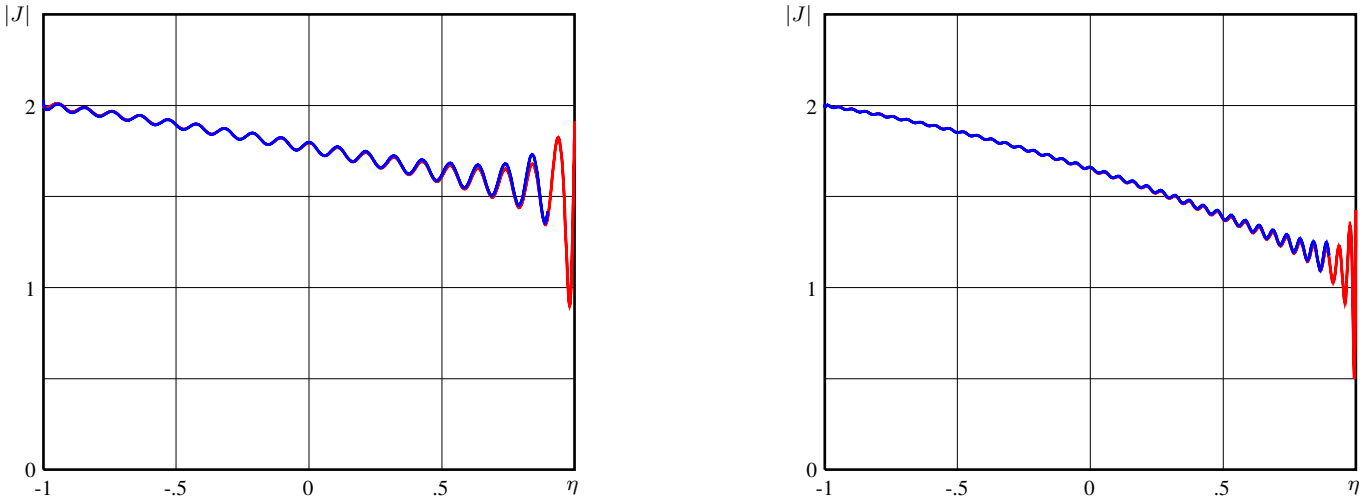

Fig. 8. Amplitudes of the induced current on the spheroid no. 3 (FEM – red, asymptotics – blue).

$$\frac{\partial\psi}{\partial y}=\frac{1}{a\sqrt{1-\eta^2}}\left(\left(2\frac{\partial\psi}{\partial\tau}-i\chi\eta\psi\right)\sin\varphi+\frac{\partial\psi}{\partial\varphi}\cos\varphi\right).$$

The substitution of the above expressions to the formula for $\mathbf{\Psi}$ yields

$$\Psi_x=-\frac{b}{4\pi}\int\limits_{-1}^{1}d\eta\int\limits_{0}^{2\pi}d\varphi\left\{\left(2\frac{\partial E_\varphi}{\partial\tau}-\frac{\partial H_\varphi}{\partial\varphi}\right)\psi\cos\varphi - H_\varphi\left(2\frac{\partial\psi}{\partial\tau}\sin\varphi+\frac{\partial\psi}{\partial\varphi}\cos\varphi\right)\right\},$$

$$\Psi_y=-\frac{b}{4\pi}\int\limits_{-1}^{1}d\eta\int\limits_{0}^{2\pi}d\varphi\left\{\left(2\frac{\partial E_\varphi}{\partial\tau}-\frac{\partial H_\varphi}{\partial\varphi}\right)\psi\sin\varphi + H_\varphi\left(2\frac{\partial\psi}{\partial\tau}\cos\varphi-\frac{\partial\psi}{\partial\varphi}\sin\varphi\right)\right\}.$$

Next, we compute the integrals in φ. The subintegral terms contain products of three trigonometric functions. Evidently the non-zero contributions are due to terms containing the products of three cosines, or two sines and one cosine with $|m-n|=1$. One can show that in view of the symmetry of the problem, the following formulas hold :

$$\Psi_x^{\mathrm{TE}}=\sum_{n=0}^{+\infty}\Psi_{nx}^{\mathrm{TE}}\cos(n\varphi_0),\qquad \Psi_y^{\mathrm{TE}}=\sum_{n=1}^{+\infty}\Psi_{ny}^{\mathrm{TE}}\sin(n\varphi_0),$$

$$\Psi_x^{\mathrm{TM}}=\sum_{n=1}^{+\infty}\Psi_{nx}^{\mathrm{TM}}\sin(n\varphi_0),\qquad \Psi_y^{\mathrm{TM}}=\sum_{n=0}^{+\infty}\Psi_{ny}^{\mathrm{TM}}\cos(n\varphi_0).$$

For the harmonics we get

$$\Psi_{nx}=-\frac{b}{4}\int\limits_{-1}^{1}\left\{\psi_n\left(\frac{\partial}{\partial\tau}+\frac{1}{2}\right)(E_{n+1}+E_{n-1}) \pm(H_{n+1}-H_{n-1})\left(\frac{\partial}{\partial\tau}+\frac{1}{2}\right)\psi_n\right\}d\eta,$$

$$\Psi_{ny}=-\frac{b}{4}\int\limits_{-1}^{1}\left\{\psi_n\left(\frac{\partial}{\partial\tau}+\frac{1}{2}\right)(E_{n+1}-E_{n-1}) \pm(H_{n+1}+H_{n-1})\left(\frac{\partial}{\partial\tau}+\frac{1}{2}\right)\psi_n\right\}d\eta$$

with the plus signs used for the TM incident wave and the minus signs to be used for the TE case.

When substituting the expressions (40) through (43) the terms with the indexes $n-2$ and $n+2$ appear in these formulas. With the help of the boundary conditions (27), (28) these terms can be excluded. Furthermore, we change the order of integration and use the formula

$$\int\limits_{-1}^{1}\left(\frac{1-\eta}{1+\eta}\right)^{i(t-s)}\frac{d\eta}{1-\eta^2}=\pi\delta(t-s),$$

which reduces the integration by s and results in the compensation of the terms containing Whittaker functions $M_{it,n/2}(-i\chi)$, implying that the incident field gives no conrtibution. In the other terms the Wronskians of Whittaker functions (47) are separated, and after substituting the expressions given in (36), we get

$$\Psi_{nx}^{\mathrm{TE}}=\frac{ib(-1)^{n+1}}{\pi(n!)^3\beta\beta_0}\int\limits_{-\infty}^{+\infty}\Gamma^2\left(\frac{n+1}{2}+it\right)\Gamma\left(\frac{n+1}{2}-it\right)\times \times M_{it,n/2}(i\beta^2)M_{it,n/2}(i\beta_0^2)\left(T_{n-1}^{\mathrm{TE}}+R_{n+1}^{\mathrm{TE}}\right)dt, \quad (61)$$

$$\Psi_{ny}^{\mathrm{TE}}=\frac{ib(-1)^{n}}{\pi(n!)^3\beta\beta_0}\int\limits_{-\infty}^{+\infty}\Gamma^2\left(\frac{n+1}{2}+it\right)\Gamma\left(\frac{n+1}{2}-it\right)\times \times M_{it,n/2}(i\beta^2)M_{it,n/2}(i\beta_0^2)\left(T_{n-1}^{\mathrm{TE}}-R_{n+1}^{\mathrm{TE}}\right)dt, \quad (62)$$

$$\Psi_{nx}^{\mathrm{TM}}=\frac{ib(-1)^{n+1}}{\pi(n!)^3\beta\beta_0}\int\limits_{-\infty}^{+\infty}\Gamma^2\left(\frac{n+1}{2}+it\right)\Gamma\left(\frac{n+1}{2}-it\right)\times \times M_{it,n/2}(i\beta^2)M_{it,n/2}(i\beta_0^2)\left(T_{n-1}^{\mathrm{TM}}-R_{n+1}^{\mathrm{TM}}\right)dt, \quad (63)$$

$$\Psi_{ny}^{\mathrm{TM}}=\frac{ib(-1)^{n}}{\pi(n!)^3\beta\beta_0}\int\limits_{-\infty}^{+\infty}\Gamma^2\left(\frac{n+1}{2}+it\right)\Gamma\left(\frac{n+1}{2}-it\right)\times \times M_{it,n/2}(i\beta^2)M_{it,n/2}(i\beta_0^2)\left(T_{n-1}^{\mathrm{TM}}+R_{n+1}^{\mathrm{TM}}\right)dt. \quad (64)$$

In the above formulas we have used the fact that $T_{-1}^{\mathrm{TE}}\equiv 0$ and $T_{-1}^{\mathrm{TM}}\equiv 0$.

We substitute the expressions (44) through (46) and (48), for the reflection coefficients in the expressions given in (61) throught (63), and rewrite Whittaker functions in terms of the Coulomb wave functions. These very cumbersome, but straightforward derivations result in the following final expressions for the far field amplitudes of the magnetic vector:

$$\Psi_x^{\mathrm{TE}}=\frac{8ib}{\pi\beta\beta_0}\int\limits_{-\infty}^{+\infty}\left\{c_0+d_0+(b^{\mathrm{TE}}+c_1+d_1)\cos\varphi + \sum_{\ell=2}^{+\infty}(a_\ell+b_\ell+c_\ell+d_\ell)\cos(\ell\varphi)\right\}dt, \quad (65)$$

$$\Psi_y^{\mathrm{TE}}=\frac{8ib}{\pi\beta\beta_0}\int\limits_{-\infty}^{+\infty}\left\{(-b^{\mathrm{TE}}+c_1+d_1)\sin\varphi + \sum_{\ell=2}^{+\infty}(-a_\ell-b_\ell+c_\ell+d_\ell)\sin(\ell\varphi)\right\}dt, \quad (66)$$

$$\Psi_x^{\mathrm{TM}}=\frac{8ib}{\pi\beta\beta_0}\int\limits_{-\infty}^{+\infty}\left\{(-b^{\mathrm{TM}}+c_1+d_1)\cos\varphi + \sum_{\ell=2}^{+\infty}(a_\ell-b_\ell+c_\ell-d_\ell)\sin(\ell\varphi)\right\}dt, \quad (67)$$

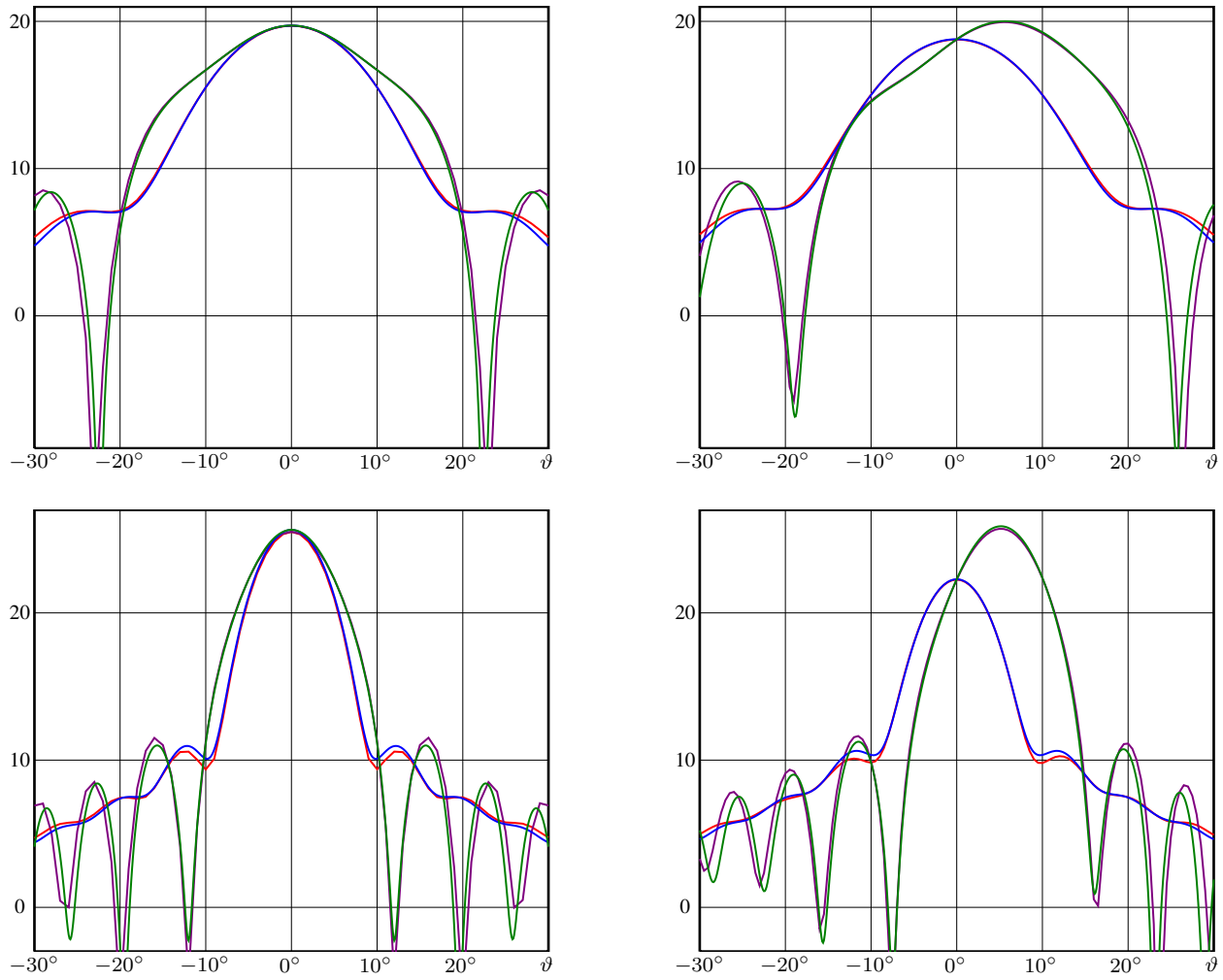

Fig. 9. The RCS (in dB) for the spheroid no. 1 at 1GHz (upper) and 2GHz (lower) for the axial incidence (left) and for the TM wave incident at $\vartheta = 5^\circ$ (right).

$$\Psi_y^{\mathrm{TM}} = -\frac{8ib}{\pi\beta\beta_0}\int\limits_{-\infty}^{+\infty}\Bigg\{c_0 - d_0 + (b^{\mathrm{TM}} + c_1 - d_1)\cos\varphi - \sum_{\ell=2}^{+\infty}(a_\ell - b_\ell - c_\ell + d_\ell)\cos(\ell\varphi)\Bigg\}dt. \quad (68)$$

Here

$$a_\ell = F_{(\ell-1)/2}\left(t, \frac{1}{2}\beta^2\right) F_{(\ell-3)/2}\left(t, \frac{1}{2}\beta_0^2\right)\frac{1}{z_{\ell-1}},$$

$$b^{\mathrm{TE}} = F_0\left(t, \frac{1}{2}\beta^2\right) F_0\left(t, \frac{1}{2}\beta_0^2\right)\frac{F_0\left(-t, \frac{1}{2}\chi\right)}{H_0^+\left(-t, \frac{1}{2}\chi\right)},$$

$$b^{\mathrm{TM}} = F_0\left(t, \frac{1}{2}\beta^2\right) F_0\left(t, \frac{1}{2}\beta_0^2\right)\frac{\dot{F}_0\left(-t, \frac{1}{2}\chi\right)}{\dot{H}_0^+\left(-t, \frac{1}{2}\chi\right)},$$

$$b_\ell = F_{\frac{\ell-1}{2}}\left(t, \frac{1}{2}\beta^2\right) F_{\frac{\ell-1}{2}}\left(t, \frac{1}{2}\beta_0^2\right)\frac{y_{\ell-1}}{z_{\ell-1}},$$

$$c_\ell = F_{\frac{\ell-1}{2}}\left(t, \frac{1}{2}\beta^2\right) F_{\frac{\ell-1}{2}}\left(t, \frac{1}{2}\beta_0^2\right)\frac{y_\ell}{z_\ell},$$

$$d_\ell = F_{\frac{\ell-1}{2}}\left(t, \frac{1}{2}\beta^2\right) F_{\frac{\ell+1}{2}}\left(t, \frac{1}{2}\beta_0^2\right)\frac{1}{z_\ell},$$

$$y_\ell = H^+_{\frac{\ell-1}{2}}\left(-t, \frac{1}{2}\chi\right)\dot{F}_{\frac{\ell+1}{2}}\left(-t, \frac{1}{2}\chi\right) + \dot{H}^+_{\frac{\ell-1}{2}}\left(-t, \frac{1}{2}\chi\right) F_{\frac{\ell+1}{2}}\left(-t, \frac{1}{2}\chi\right),$$

$$z_\ell = H^+_{\frac{\ell-1}{2}}\left(-t, \frac{1}{2}\chi\right)\dot{H}^+_{\frac{\ell+1}{2}}\left(-t, \frac{1}{2}\chi\right) + \dot{H}^+_{\frac{\ell-1}{2}}\left(-t, \frac{1}{2}\chi\right) H^+_{\frac{\ell+1}{2}}\left(-t, \frac{1}{2}\chi\right).$$

We illustrate the approximating properties of the above asymptotics by comparing the RCS

$$\mathrm{RCS} = 4\pi\|\mathbf{\Psi}\|^2$$

computed by using these formulas and with the help of HFSS of ANSYS[1]. For this purpose, we choose the same test

[1]Computations were performed by D. Shevnin, CADFEM CIS Branch in North-West Federal Region.

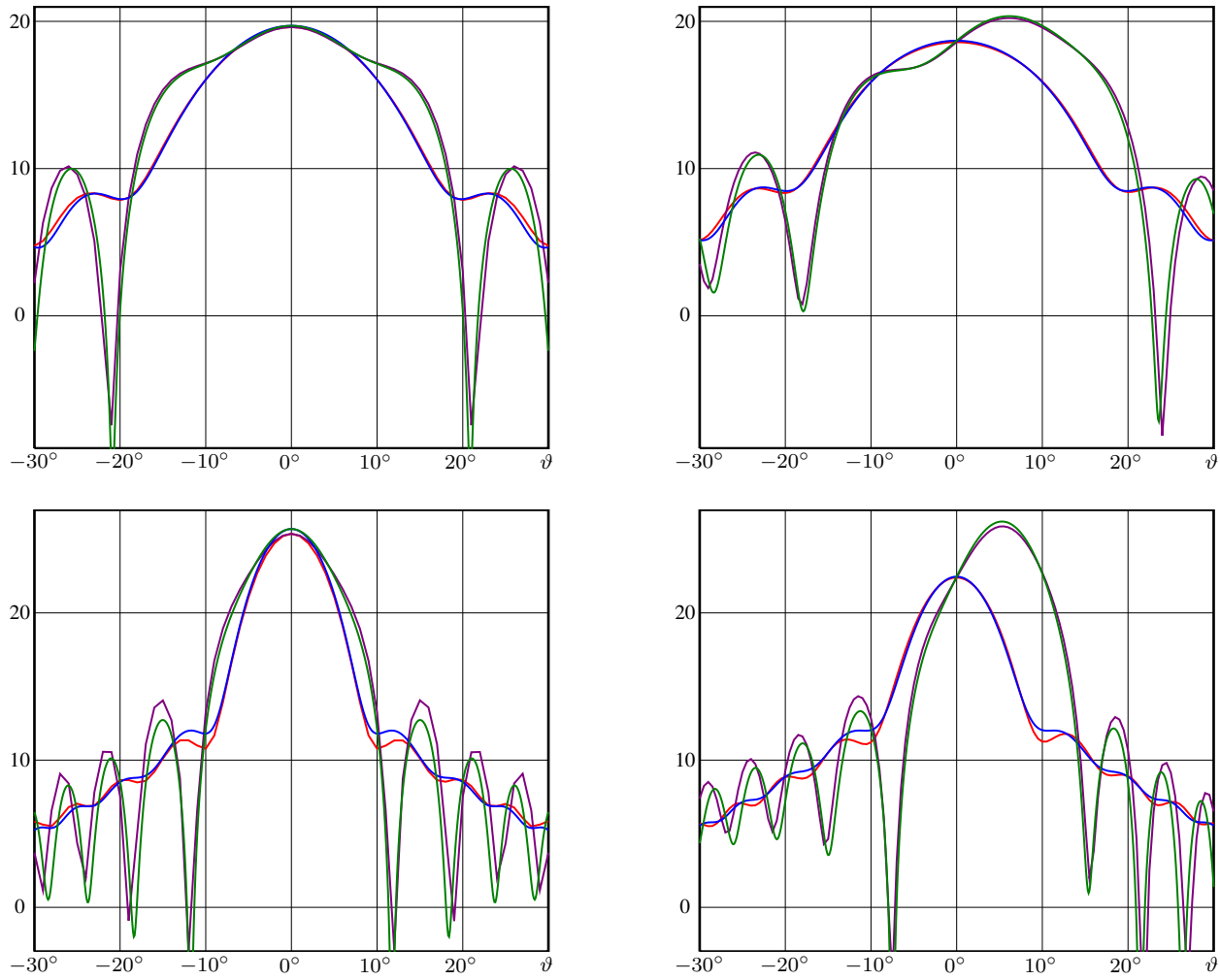

Fig. 10. The RCS (in dB) for the spheroid no. 2 at 1GHz (upper) and 2GHz (lower) for the axial incidence (left) and for the TM wave incident at $\vartheta = 5^\circ$ (right).

problems as specified in Table I. Red and magenta colours are used in the Figs. 9 through 11 to identify the results of numerical computations and green and blue curves correspond to the asymptotic results.

G. The total scattering cross-section

The formulas (65) throught (68) provide the asymptotics of the far field amplitude of the magnetic field under the assumption that the angles ϑ and ϑ_0 are small, i.e., the directions of the incidence and of the observation are in narrow cones near the axis of the body. Nevertheless, these formulas enable us to find the total scattering cross-section $\sigma(\vartheta_0)$. According to the "optical" theorem [3] we have

$$\sigma(\vartheta_0) = \frac{4\pi}{k}\mathrm{Im}\,\langle \mathbf{\Psi}(\vartheta_0, \vartheta_0, 0), \mathbf{h}\rangle\,, \tag{69}$$

where $\mathbf{h}$ is the magnetic polarization vector of the incident wave and the angular brackets denote scalar product.

The magnetic vector is directed along $-\mathbf{e}_x$ in the TE case and along $\mathbf{e}_y$ in the TM case. Therefore, we have, $\left\langle \mathbf{\Psi}^{+1}, \mathbf{h}^{+\mathbf{1}}\right\rangle = -\Psi_x^{+1}$, $\left\langle \mathbf{\Psi}^{-1}, \mathbf{h}^{-\mathbf{1}}\right\rangle = \Psi_y^{-1}$.

To exclude the dependence of the effective cross-section on the size of the spheroid we normalize it by the visible cross-section $\sigma_0 = \pi a^2\sqrt{1+\beta_0^2/\chi}$ and define $\Sigma = \sigma/\sigma_0$. Then

$$\Sigma^{\mathrm{TE}} = -\frac{32}{\pi\chi\beta^2\sqrt{1+\beta_0^2/\chi}}\times \\ \times\sum_{n=0}^{+\infty}\mathrm{Im}\int_{-\infty}^{+\infty}\left\{b^{\mathrm{TE}} + \sum_{\ell=0}^{+\infty}(b_{\ell+2} + c_\ell + 2d_\ell)\right\}dt, \tag{70}$$

$$\Sigma^{\mathrm{TM}} = -\frac{32}{\pi\chi\beta^2\sqrt{1+\beta_0^2/\chi}}\times \\ \times\sum_{n=0}^{+\infty}\mathrm{Im}\int_{-\infty}^{+\infty}\left\{b^{\mathrm{TM}} + \sum_{\ell=0}^{+\infty}(b_{\ell+2} + c_\ell - 2d_\ell)\right\}dt. \tag{71}$$

For the case of $\beta = 0$, the representations (70) and (71) contain an ambiguity, and by avoiding it we conclude that the only nonzero term is c_0. The formulas then simplify and lose the dependence on the polarization of the incident wave;

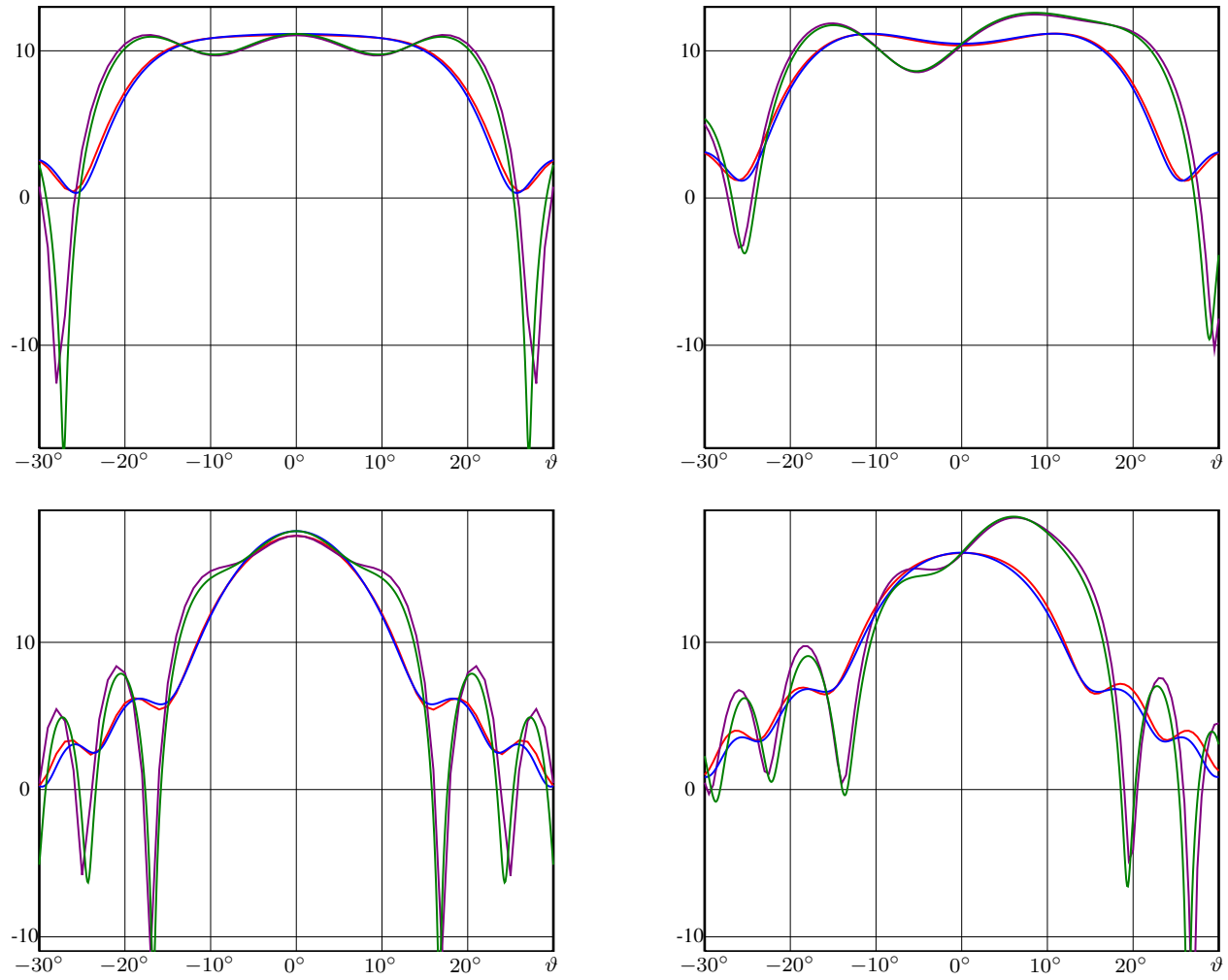

Fig. 11. The RCS (in dB) for the spheroid no. 3 at 1GHz (upper) and 2GHz (lower) for the axial incidence (left) and for the TM wave incident at $\vartheta = 5^\circ$ (right).

hence, we have

$$\Sigma = -\frac{16}{\chi}\mathrm{Im}\left\{\int_{-\infty}^{+\infty}\frac{y_0}{z_0}\frac{d\lambda}{1+e^{2\pi\lambda}}\right\}. \qquad (72)$$

The dependencies of the total scattering cross-section on the parameter of elongation χ are presented in Fig. 12. We see that the rate of elongation may significantly affect the value of the scattering cross-section. As χ grows, and the body becomes less elongated, the effective cross-section tends to its classical high-frequency limit of two.

V. Conclusion

For elongated bodies, the induced currents of the forward wave generate the far field amplitudes in the forward cone near the axis. For larger observation angles ϑ, it is necessary to consider the currents near the ends of the body. However for $\vartheta \approx \pi$ the main contribution to $\mathbf{\Psi}$ again comes from the currents in the middle part of the spheroids, however the backward wave plays a role in this case. The other contribution to the back-scattered field is due to the specular reflection. The contribution of the specular point and that of the backward wave can both be found in the framework of the approach presented in this paper. For the case of acoustic waves, this has been done in [27].

In addition to spheroids, some other types of elongated bodies can also be considered. The parabolic equations enable us to use the separation of variables for the case in which the quantity $\rho_t(s)\rho^{-1/3}(s)$ is constant. This is the case for spheroids, hyperboloids, paraboloid and surfaces that have no curvature: cones and cylinders that have been analyzed in [28]. The case of a paraboloid does not give any new results compared to those of Fock [2]. For the one-sheeted hyperboloid, some results have been presented in [29]. The case of a narrow cone has been studied in [30]. Besides the bodies of revolution one can consider infinite cylinders with a strongly elongated cross-section. For this case, the electromagnetic problems reduce to scalar diffraction and the results of [31] are applicable.

We have considered only the case of plane wave incidence, however other sources are possible. For the case of an acoustic point source the reader is referred to [32]. The other possibility

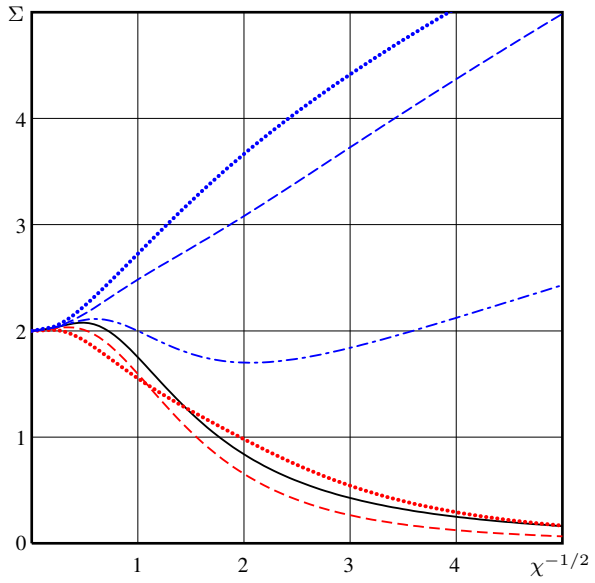

Fig. 12. The total scattering cross-section as a function of the elongation parameter χ. Solid black line is for $\beta = 0$, dash-dotted — for $\beta = 0.5$, dashed — for $\beta = 1$, dotted — for $\beta = 2$. Red is for the TE case and blue is for the TM case.

is to consider Gaussian beams incident on an elongated body.

All the above listed possible directions of further research are almost straightforward although they do require derivations that are rather cumbersome.

The other, and more difficult questions pertain to the following two aspects. The first of these is the generalization of this technique to the case of the impedance boundary condition, making it possible for it to handle dielectric bodies. The difficulty here comes from the use the τ coordinate which is related to the normal n by the formula

$$\frac{\partial}{\partial \tau} = \frac{1}{2a\sqrt{1-\eta^2}} \frac{\partial}{\partial n},$$

which contains η. The second challenge is to apply the approach to bodies whose shapes are not close to one of the canonical surfaces, but are composed of parts each of which can be approximated by a canonical surface. For example, the ogival geometry can be considered as a combination of circular cones at the ends and a spheroid in the middle part. We note that while asymptotic representations for the diffracted fields by cones and spheroids are known, the issue of their matching remains an open question.

References

[1] V. A. Fock "The distribution of currents induced by a pane wave on the surface of a conductor", *Journ. of Phys. of the USSR*, vol. 10, no. 2, pp. 130–136, 1946.

[2] V. A. Fock "Theory of diffraction from the paraboloid of revolution", in *Diffraction of electromagnetic waves by some bodies of revolution*, Moscow, Sovetskoe Radio, pp. 5–56, in Russian, 1957.
see also V. A. Fock *Electromagnetic Diffraction and Propagation Problems*, (International Series of Monographs on Electromagnetic Waves), Frankfurt, Pergamon Press, Chapter 3, 1965.

[3] H. Hönl, A. W. Maue, K. Westpfahl *Theorie der Beugung*, Springer-Verlag, Berlin–Göttingen–Heidelberg, 1961.

[4] R. W. P. King, T. T. Wu *The scattering and diffraction of waves*, Harward Univ. Press. Cambridge, Massachusetts, 1959.

[5] M.G. Belkina, L.A. Wainstein "The characteristics of radiation of spherical surface antennas", in *Diffraction of electromagnetic waves by some bodies of revolution*, Moscow, Sovetskoe Radio, pp. 57–125, in Russian, 1957.

[6] S. Hong "Asymptotic theory of electromagnetic and acoustic diffraction by smooth convex surfaces of variable curvature", *Journal of Mathematical Physics*, vol. 8, no. 6, p. 1223–1232, 1967.

[7] I. V. Andronov, D. Bouche "Computation of the second order term for the propagation parameter of creeping waves by boundary layer method" *Annales des Télécommunications*, vol. 49, no. 3–4, pp. 193–210, 1994.

[8] V. I. Ivanov "Computation of corrections to the Fock asymptotics for the wave field near a circular cylinder and a sphere", *J. of Soviet Mathematics*, vol. 20, no. 1, pp. 1812–1817, 1982.

[9] I. V. Andronov, D. P. Bouche, M. Duruflé "High-frequency diffraction of plane electromagnetic wave by an elongated spheroid", *IEEE Transactions on Antennas and Propag.*, vol. 60, no. 11, pp. 5286–5295, 2012.

[10] T. B. A. Senior "Disk scattering at edge-on incidence", *IEEE Trans Antennas Propag*, vol. 17, no. 6, pp. 751–756, 1969.

[11] T. B. A. Senior "Loop excitation of travelling waves", *Can J Phys*, vol. 40, pp. 1736, 1962.

[12] T. S. Bird "Comparison of Asymptotic Solutions for the Surface Field Excited by a Magnetic Dipole on a Cylinder", *IEEE Transactions on Antennas and Propagation*, vol. AP-32, no. 11, pp. 1237–1244, 1984.

[13] I. V. Andronov, D. Bouche "Asymptotic of creeping waves on a strongly prolate body, *Ann. Télécommun.*, vol. 49, no. 3–4, pp. 205–210, 1994.

[14] F. Molinet, I. V. Andronov, D. Bouche *Asymptotic and hybrid methods in electromagnetics*, IEE, London, 2005.

[15] J. C. Engineer, J. R. King, R. H. Tew "Diffraction by slender bodies", *Eur J Appl Math*, vol. 9, no. 2, pp. 129–158, 1998.

[16] S. Yu. Slavyanov, W. Lay, A. Seeger "The classification of Heun's equation and its special nd confluent cases", in A. Ronveaux (Ed.) *Heun equation*, Oxford University Press, Oxford, 1995.

[17] F. A. Molinet "Plane wave diffraction by a strongly elongated object illuminated in the paraxial direction", em Progress in Electromagnetics Research B, vol. 6, pp. 135–151, 2008.

[18] N. Ya. Kirpichnikova, M. M. Popov "The Leontovich-Fock Parabolic Equation Method in Problems of Short-Wave Diffraction by Prolate Bodies", *Journal of Mathematical Sciences*, vol. 194, no. 1, pp. 30–43, 2012.

[19] I. V. Andronov "High-frequency Asymptotics for Diffraction by a Strongly Elongated Body", *Antennas and Wireless Propagation Letters*, vol. 8, p. 872, 2009.

[20] I. V. Andronov "High frequency asymptotics of electromagnetic field on a strongly elongated spheroid", *PIERS Online*, vol. 5, no. 6, pp. 536–540, 2009.

[21] I. V. Komarov, L. I. Ponomarev, S. Yu. Slavyanov *Spheroidal and Coulomb Spheroidal Functions*, Nauka, Moscow, in Russian, 1976.

[22] M. Abramowitz, I. Stegun *Handbook of mathematical functions*, National Bureau of Standards, New York, 1964.

[23] I. V. Andronov "The currents induced by a high-frequency wave incident at a small angle to the axis of strongly elongated spheroid", *Progress in Electromagnetics Research M*, vol. 28, pp. 273–287, 2013.

[24] I. J. Thompson, A. R. Barnett "COULCC: A continued-fraction algorithm for Coulomb functions of complex order with complex arguments", *Computer Physics Communications*, vol. 36, pp. 363–372, 1985.

[25] I. V. Andronov, D. Bouche "Forward and backward waves in high-frequency diffraction by an elongated spheroid", *Progress in Electromagnetics Research B*, vol. 29, pp. 209–231, 2011.

[26] J. A. Stratton, L. J. Chu "Diffraction theory of electromagnetic waves", *Phys. Review*, vol. 56, no. 1, pp. 99–107, 1939.

[27] I. V. Andronov "High-frequency acoustic scattering from prolate spheroids with high aspect ratio", *Journal of the Acoustical Soc. Am.*, vol. 134, no. 6, pp. 4307–4316, 2013.

[28] I. V. Andronov "Calculation of Diffraction by Strongly Elongated Bodies of Revolution", *Acoustical Physics*, vol. 58, no. 1, pp. 22–29, 2012.

[29] I. V. Andronov "The influence of large transverse curvature on the induced currents attenuation", *Antennas and Wireless Propag. Letters*, vol. 11, p. 121, 2012.

[30] I. V. Andronov, D. Bouche "Diffraction by a narrow circular cone as by a strongly elongated body", *Journal of Mathematical Sciences*, vol. 185, no. 4, pp. 517–522, 2012.

[31] I. V. Andronov "Diffraction by elliptic cylinder with strongly elongated cross-section", *Acoustical Physics*, vol. 60, no. 3, to be published, 2014.

[32] I. V. Andronov "Diffraction of spherical waves on large strongly elongated spheroids", *Acta Acoustica united with Acoustica*, vol. 99, no. 2, pp. 177–182, 2013.